von Hippel Lindau tumor suppressor regulates hepatic glucose metabolism by controlling expression of glucose transporter 2 and glucose 6-phosphatase

SANG-KI PARK[1,3], VOLKER H. HAASE[2] and RANDALL S. JOHNSON[1]

[1]Molecular Biology Section, Division of Biological Sciences, University of California, San Diego, La Jolla, CA 92093-0366; [2]Renal-Electrolyte and Hypertension Division, Department of Medicine, University of Pennsylvania, Philadelphia, PA 19104-6144; [3]Department of Pharmaceutical Sciences, St. John's University, Queens, NY 11439, USA

Received September 5, 2006; Accepted October 25, 2006

Abstract. von Hippel Lindau (VHL) disease is a hereditary cancer syndrome caused by biallelic inactivation of the *VHL* tumor suppressor gene. The most widely known function of VHL is to limit normoxic protein expression of hypoxia-inducible factor-α (HIF-α). Loss of the functional VHL gene causes constitutive stabilization of HIF-α that primarily up-regulates hypoxia-inducible genes even at normal oxygen concentration, which in turn contribute to VHL tumor progression. We report on the novel function of VHL in hepatic glucose storage and disposal. VHL deletion in adult mouse liver quickly leads to increased accumulation of glycogen granules as well as lipid droplets. This abnormal glycogen storage in VHL-inactivated liver arises at least in part from significantly reduced expression of two key liver-specific glucose metabolism genes, glucose transporter-2 (GLUT2) and glucose-6-phosphatase (G-6-Pase). The expression pattern of these genes in VHL knock-out liver was in contrast to that of well-known HIF target genes, such as PGK, Glut-1, VEGF, and EPO, all of which are highly elevated upon VHL inactivation. Our findings suggest that two distinct signaling pathways exist at the downstream of VHL controlling different sets of gene expression. Following VHL inactivation, one pathway causes oxygen-independent overexpression of classic hypoxia-inducible genes and the other one described here suppresses expression of the genes important for liver glucose metabolism.

Correspondence to: Dr Sang-ki Park, Department of Pharmaceutical Sciences, College of Pharmacy and Allied Health Profession, St. John's University, 8000 Utopia Parkway, Queens, NY 11439, USA
E-mail: parks@stjohns.edu

Abbreviations: pVHL, von Hippel Lindau protein; HIF, hypoxia-inducible factor; GLUT, glucose-transporter; G-6-Pase, glucose-6-phosphatase; HRE, hypoxia-responsive element; RCC, renal cell carcinoma; RT, reverse transcriptase

Key words: pVHL, HIF, glycogen, tumor cell metabolism, gene expression

Introduction

von Hippel Lindau (VHL) disease is a hereditary cancer syndrome that predisposes the affected individuals to develop various types of tumors, such as hemangioblastomas in the central nervous system and retina, clear-cell carcinoma in the kidney, cystadenomas in the pancreas and testis, and pheochromocytoma in the adrenal gland (1). Tumor development in these patients is linked to heterozygous germ line mutation in the VHL tumor suppressor gene and subsequent somatic inactivation or loss of the remaining wild-type allele (1,2). The most extensively characterized function of pVHL is its ability to recruit hypoxia-inducible factor (HIF)-α for multiple rounds of conjugation with ubiquitins in an oxygen-dependent manner (2). Polyubiquitinated HIF-α is destined to be destroyed by 26S-proteasome, hence HIF-α is barely detectable in most cells under normal oxygen concentration, whereas it quickly accumulates in hypoxic cells (3-5). The stabilized HIF-α dimerizes with HIF-1ß to form a functional transcription factor (HIF) that coordinates diverse cellular adaptation processes to hypoxia primarily by stimulating expression of genes involved in angiogenesis, glycolysis, and blood oxygen transport, etc. (3). Biallelic inactivation of VHL leads to normoxic stabilization and activation of HIF-α and concurrent induction of HIF target genes, such as phosphoglycerate kinase (PGK), glucose transporter 1 (GLUT-1), vascular endothelial growth factors/vascular permeability factor (VEGF/VPF) (2). Elevated expression of these HIF target genes in turn constitutes molecular changes and morphological characteristics of VHL syndromes. For instance, VHL-deficient cells produce significantly elevated amount of VEGF independent of oxygen concentration, which probably accounts for the high density vasculature commonly observed in VHL tumors and can be reversed by reintroduction of wild-type VHL (6,7). VHL inactivation is associated with the clear-cell variant of RCC, accounting for approximately 75% of all sporadic clear cell renal carcinomas (8). In contrast to human RCC, clear cell kidney tumor is rare for the rat but can be induced by oral administration of $KBrO_3$ (9). This chemical-induced clear cell RCC also strongly correlates with inactivating mutation of VHL (9). Clear cell appearance of VHL tumors is not limited to the cells of

Table I. Sequences of primers used for real-time PCR analysis.

Gene	Primers	Product size (bp)	GeneBank
VHL	FP: 5'-CTGCCTTTGTGGCTCAACTT-3' RP: 5'-TGACGATGTCCAGTCTCCTG-3'	292	NM_009507
EPO	FP: 5'-CTCCACTCCGAACACTCACA-3' RP: 5'-CCTCTCCCGTGTACAGCTTC -3'	96	NM_007942
GLUT-2	FP: 5'-GCCTGTGTATGCAACCATTG-3' RP: 5'-GAAGATGGCAGTCATGCTCA-3'	205	NM_031197
G-6-Pase	FP: 5'-TCTGTCCCGGATCTACCTTG-3' RP: 5'-GTAGAATCCAAGCGCGAAAC-3'	172	NM_008061

kidney nephron origin, but is also found in papillary cystadenoma of the epididymis and microcystic adenomas of the pancreas in VHL patients (8,9). However, it is not clear whether the lack of cytoplasmic staining is a direct consequence of VHL deletion in those cells or results indirectly from systemic adaptations that have accumulated over a long period of time following VHL inactivation. In addition, molecular mediators accountable for this change remain unidentified. With an inducible VHL knock-out mouse model, we demonstrated that the clear cell phenotype can be recapitulated shortly after VHL deletion in the liver of the adult animals. We also demonstrated that the morphological changes in VHL-inactivated hepatocytes result from significantly increased accumulation of glycogen granules as well as lipid droplets. Furthermore, we identified two glycogen metabolizing genes, glucose transporter 2 (GLUT2) and glucose-6-phosphatase (G-6-Pase), as pVHL downstream targets that are likely responsible for deregulated glycogen storage in the VHL-inactivated liver. In contrast to well-known VHL target genes whose expression is positively regulated by HIF upon VHL inactivation, expression of GLUT2 and G-6-Pase genes is significantly decreased in VHL-inactivated hepatocytes. Down-regulation of these two liver-specific glucose metabolizing genes by VHL deletion may represent new as-yet unidentified VHL functions.

Materials and methods

Generation of mice and inducible deletion of the VHL gene in the liver. All animal procedures were performed according to protocols approved by the University of California San Diego Animal Care and Use Committees. Mice that carried the conditional loxP alleles, *VHL* alleles flanked by loxP sites ($VHL^{+F/+F}$), were generated by engineering a loxP site in the promoter and a loxP-flanked NeoR cassette in the first intron as described previously (10). The targeted allele was crossed into a transgenic mouse line expressing Cre recombinase under the control of interferon α/ß-inducible promoter of the mouse Mx gene (a gift from Dr Rajewsky) (11). These mice were intraperitoneally injected with a single dose of 300 μl of 1 mg/ml pIpC (Amersham Biosciences, Piscataway, NJ). To minimize the confounding effects due to anti-viral defensive effects of pIpC, both control and knock-out mice were administered with pIpC. Controls were in all cases littermates that were genotyped as containing only the loxP-flanked VHL allele with no Mx-cre transgene.

Genotyping and determination of extent of VHL deletion. Genotyping for loxP flanked VHL exon 1 and Mx-cre were performed using PCR with genomic DNA isolated from snipped tail of mice at 4 weeks of age, as described previously (12). The degree of excision was calculated by comparing VHL exon 1 level relative to c-Jun DNA level in $VHL^{+F/+F}$/Mx-$Cre^{+/-}$ mouse liver with that of a wild-type counterpart. A week after pIpC injection, the livers were dissected and lysed to purify genomic DNA. Abundance of VHL exon 1 was determined by quantitative PCR analysis of the region flanked by two loxP sites with the primer set, VHL-1: 5'-CTAGGCA CCGAGCTTAGAGGTTTGCG-3', VHL-2: 5'-CTGACTTC CACTGATGCTTGTCACAG-3', using a SYBR®-Green PCR Master mix kit (Applied Biosystems), whereas the c-Jun gene level was measured with a TaqMan® Universal PCR Master mix kit, as described previously (12). PCR amplification was monitored with the ABI PRISM 7700 sequence detector (Applied Biosystems, Foster City, CA, USA).

Liver histology and immunohistochemical analysis. The livers were dissected and embedded with paraffin to prepare histology sections. Hematoxylin and eosin, and oil red staining were performed by the University of California at San Diego (UCSD) Cancer Center Histology Resource (La Jolla, CA, USA). To detect PCNA-positive cells, the sections were deparaffinized with xylene and rehydrated with graded ethanol. And then they were stained with anti-PCNA (Pharmingen, San Diego, CA) and visualized with a Vectastain ABC kit, using the chromophore 3,3-diamino-benzidine (DAB) substrate (Vector Laboratories, Burlingame, CA)

Liver glycogen assay. Liver glycogen contents were quantified as previously described with anthrone (Sigma-Aldrich, St. Louis, MO) (13). Briefly, minced liver tissues were lysed in 0.5-ml volume of 30% KOH at 100˚C for 10 min, followed by a 3-min cool down at room temperature incubation. Then, the samples were diluted (1:10) with 30% KOH and

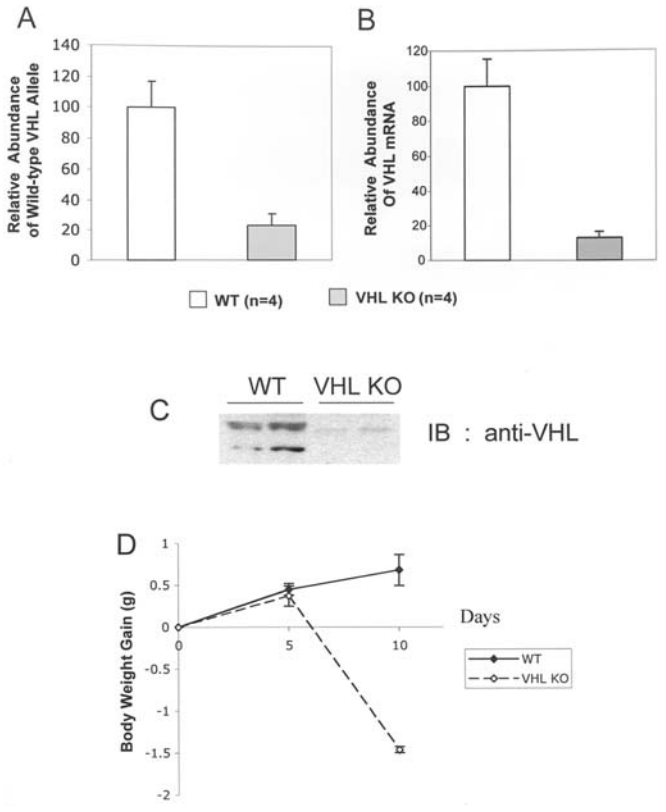

Figure 1. Inducible deletion of VHL in adult mouse liver. (A) Deletion of VHL exon 1 in $VHL^{+F/+F}MxCre^{+/-}$ mice after pIpC injection. Purified liver genomic DNAs were quantitated by SYBR®-Green-based quantitative PCR analysis. Relative abundance of VHL exon 1 was calculated against JUN allele. The values for the mean ± SEM were calculated from 4 mice for each genotype and shown in the y-axis. (B) VHL mRNA level of wild-type and VHL-deleted livers. Total RNAs were prepared and reverse transcribed to generate first-strand cDNAs. VHL mRNA content was determined by SYBR®-Green-based quantitative PCR analysis with the primer sets, 5'-CTAGGCACCGAGCTTAGAGGTTTGCG-3' and 5'-CTGACTTCCA CTGATGCTTGTCACAG-3' after normalization to the amount of ß-actin mRNA. The values for the mean ± SEM were calculated from 4 mice for each genotype and shown in the y-axis. (C) Western blot analysis of cell extracts shows significantly decreased expression of VHL in VHL-inactivated liver. (D) Body weight change following VHL deletion. Both wild-type ($VHL^{+F/+F}/MxCre^{-/-}$) and VHL knock-out ($VHL^{+F/+F}/MxCre^{+/-}$) mice were administered with pIpC on day 0 and their body weights were measured. The values for the mean ± SEM were calculated from 3 mice for each genotype and shown in the y-axis.

mixed with anhydrous ethanol. The precipitated glycogen was collected by centrifugation at 5,700 rpm for 15 min. The supernatant was carefully removed, and the pellet was resuspended in 0.5 ml of H_2O. One ml of 0.2% anthrone reagent (0.2 g in 100 ml of 98% H_2SO_4) was added, and the mixture was further incubated for 30 min. The samples were then measured at 620 nm with a spectrophotometer. A series of different concentrations of glycogen solutions were also analyzed with a similar method to generate the standard curve.

Western blot analysis. Liver tissues were collected into the liquid nitrogen and transferred to a -80˚C freezer until needed. Cell extracts were prepared from tissue lysates obtained with a Polytron benchtop homogenizer (Brinkmann Instruments, Westbury, NY) as previously described (14). A total of 50 μg of proteins were separated by SDS-PAGE and analyzed by Western blotting with a mouse anti-VHL (Pharmingen, San Diego, CA) or a rabbit anti-HIF-2α antibody (Novus Biologicals, Littleton, CO). To estimate the phosphorylation status of AKT, the transferred membrane was probed with phosphospecific anti-AKT antibody and then the same membrane was reprobed with anti-AKT (Cell Signaling Technology, Inc., Beverly, MA).

Gene expression analysis. First-strand cDNA synthesis and real-time PCR analysis was carried out as described previously (14). For real-time PCR analysis of PGK, GLUT1, and VEGF, the diluted cDNAs were amplified in the TaqMan® Universal PCR Master mix by using an ABI PRISM 7700 sequence detector (PE Applied Biosystems, Branchburg, NJ) with the primer and probe sets used in the previous study (14). The same cDNAs were used to measure the mRNA expression level of EPO, glucose-6-phosphatase, and GLUT2 by using the SYBR®-Green PCR Master mix kit (Applied Biosystems). The primer sets for the SYBR-Green PCR are shown in Table I.

Results

Histological assessment and HIF target gene expression profile of VHL-inactivated adult mouse liver. In order to inquire into the more immediate effect of VHL inactivation in tissues of fully developed animals, we generated an inducible conditional VHL knock-out mouse line. The mice carrying two loxP sites inserted into the flanking regions of the VHL exon 1 were crossed into a transgenic line that has cre-recombinase coding sequence under the control of Mx-1 promoter to generate $VHL^{+F/+F}/MxCre^{+/-}$ (10,11). These mice were allowed to maintain their wild-type VHL allele until they reached 1 to 2 months old and then their VHL exon 1 was excised out by single intraperitoneal injection of synthetic double-stranded RNA (pIpC). Gene knock-out efficiency was estimated with quantitative PCR analysis of liver genomic DNA, which showed that VHL exon 1 is deleted in approximately 80% of the liver cells in the $VHL^{+F/+F}/MxCre^{+/-}$ by a simple pharmacological treatment (Fig. 1A). The deletion efficiency of our VHL knock-out model was comparable to those described for this type of cre-recombinase transgenic mice (11). Effective gene deletion was further validated by reverse transcription-quantitative PCR (RT-qPCR) analysis with the total tissue RNA that shows >90% reduction of VHL mRNA expression in the knock-out liver compared to wild-type (Fig. 1B). Lack of expression of VHL protein (pVHL) was confirmed by Western blot analysis with anti-VHL antibody. The VHL gene is known to encode proteins with two different sizes, 30 and 19 kDa, both of which are active in regulating hypoxia-inducible factors (15), and were also detected in wild-type cytoplasm of wild-type liver but not present in the MxCre-positive liver, confirming efficient gene deletion in our animal model (Fig. 1C). Taken together, these data confirm that the $VHL^{+F/+F}/MxCre^{+/-}$ mouse with pIpC injection is a suitable animal model for the investigation of the relatively immediate effect of VHL deletion on cellular physiology, especially hepatocyte metabolism.

$VHL^{+F/+F}/MxCre^{+/-}$ mice died within approximately a month following receiving pIpC, indicating VHL is indispensable to

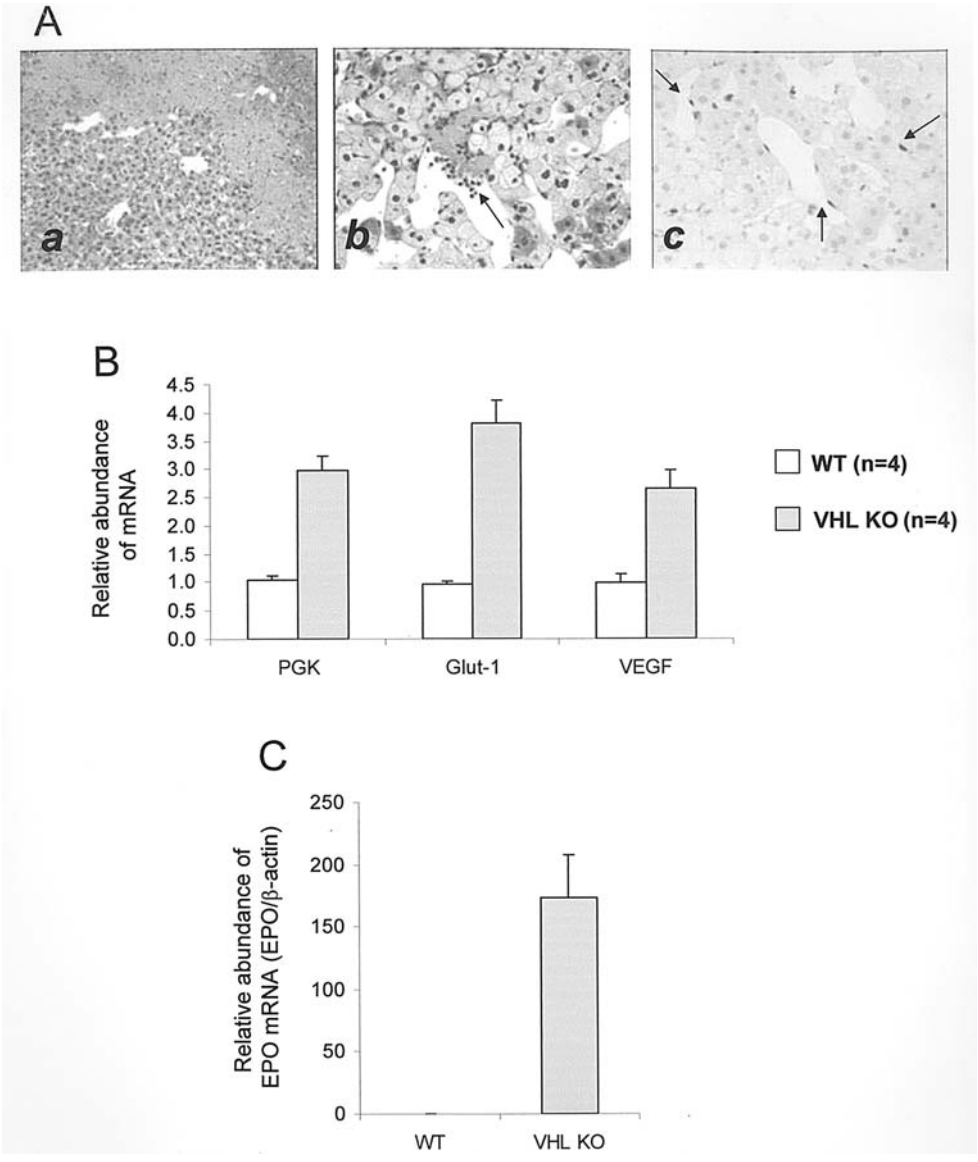

Figure 2. Effect of VHL inactivation in liver morphology and gene expression. (A) Histological changes of VHL-inactivated liver. a, development of blood-filled cavities and fibrosis in VHL-deleted liver. b, infiltration of inflammatory cells in the hepatic sinusoids near the fibrotic area (indicated in arrows). c, PCNA staining of the liver section indicates proliferation of non-parenchyma cells (indicated in arrows). (B) Gene expression changes of classic hypoxic inducible genes in VHL-deleted liver. Total liver RNA was reverse-transcribed and quantified by TaqMan-based quantitative PCR analysis. Each signal was normalized against HPRT. The values for the mean ± SEM were calculated from 4 mice for each genotype and shown in the y-axis. (C) Gene expression changes of EPO in VHL-deleted liver. EPO mRNA content was determined by SYBR®-Green-based quantitative PCR analysis with the primer sets listed in Table I. Each signal was normalized against ß-actin. The values for the mean ± SEM were calculated from 4 mice for each genotype and shown in the y-axis.

not only normal development but also to sustaining adult life (surviving days = 37.8±10.9, n=6). Death was preceded by dramatic whole body weight loss (Fig. 1D). Previous study has shown that deletion of VHL in the developing liver ($VHL^{+F/+F}$/Albumin-$Cre^{+/-}$ mice) generates blood-filled cavities and focal proliferation of small vessels, and is sufficient to trigger formation of cavernous hemangiomas from wild-type endothelial cells (10). Histological analysis showed that the $VHL^{+F/+F}$/$MxCre^{+/-}$ mouse liver quickly loses its lobular structures, mainly due to the same reasons found in $VHL^{+F/+F}$/Albumin-$Cre^{+/-}$ mice (i.e., blood-filled cavities and fibrosis) within 7 days of pIpC injection (panel a of Fig. 2A). Infiltration of the inflammatory cells into the liver sinusoid was also evident near the area undergoing fibrosis (panel b of Fig. 2A). Immunohistochemical analysis showed that the cells lining up the hepatic parenchyma are strongly stained with anti-PCNA antibody, indicating a high proliferation status of sinusoidal endothelial cells (panel c of Fig. 2A) which is again in agreement with the previously described phenotype of $VHL^{+F/+F}$/Albumin-$Cre^{+/-}$ mice. Judging from the gene deletion data, the majority of the hepatocytes (>80%) are expected to be VHL-deficient, but only very few parenchyma cells are PCNA-positive (panel c of Fig. 2A), substantiating our previous hypothesis that deletion of the VHL gene in liver parenchyma cells provides a strong growth promoting environment for endothelial cells but for themselves (10).

As expected, excision of VHL exon 1 resulted in at least several fold induction of classical HIF target genes, such as PGK, Glut-1, and VEGF in normoxic adult mouse liver (Fig. 2B). The level of EPO mRNA, which is typically below

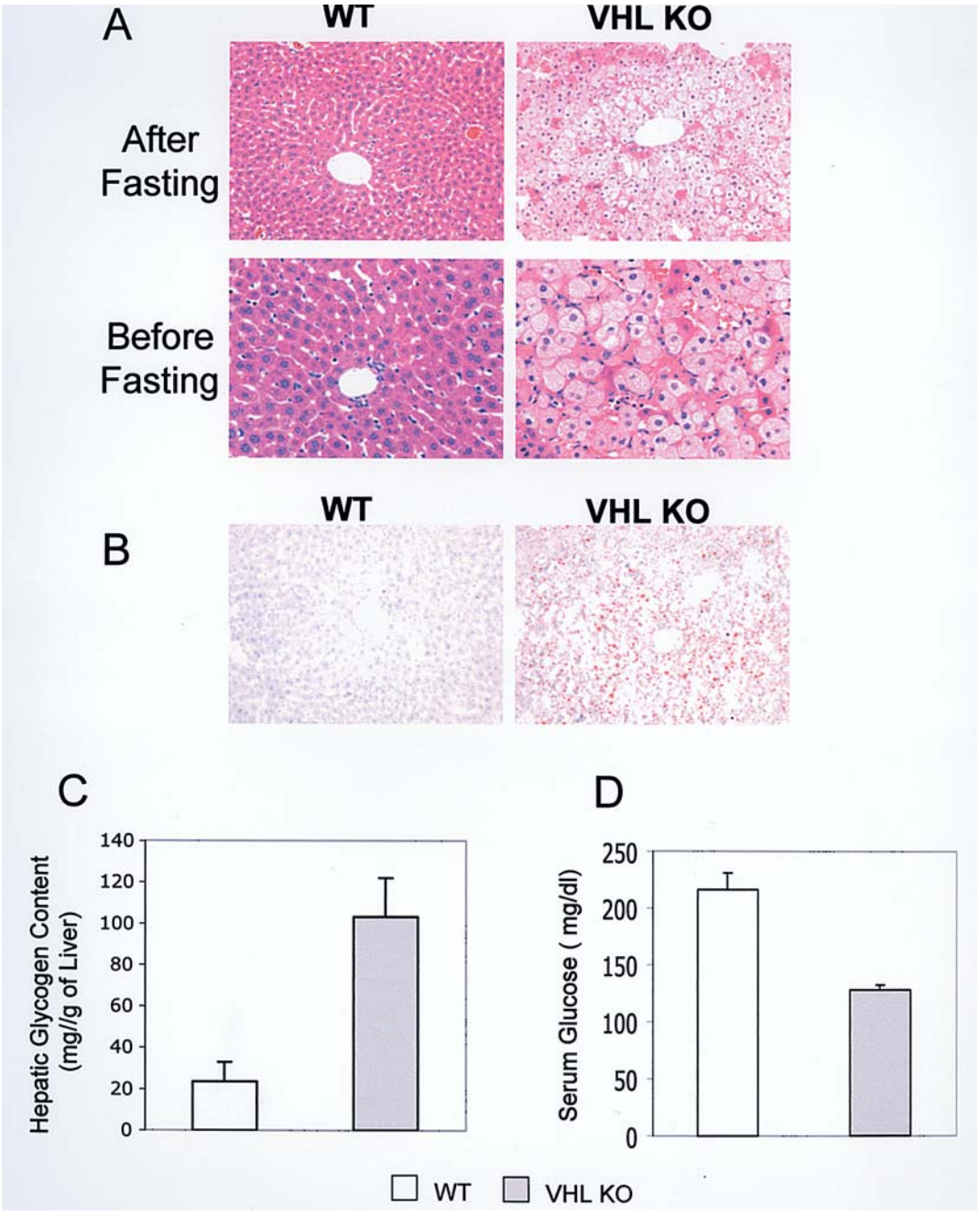

Figure 3. Increased accumulation of lipid-droplets and glycogen granules in VHL-inactivated mouse liver. (A) H&E staining of wild-type (left) and VHL knock-out (right) livers before (bottom panels) and after (top panels) fasting. (B) Oil-red O staining of wild-type (left) and VHL knock-out (right) livers. (C) Hepatic glycogen content. (D) Fasting serum glucose level in wild-type and VHL knock-out mice. The values for the mean ± SEM were calculated from 3 mice for each genotype and shown in the y-axis.

the detection limit in the wild-type liver, was dramatically elevated following VHL deletion (>150-fold over the EPO level in unstimulated wild-type kidney) (Fig. 2C).

Clear cell characteristics of VHL-deleted hepatocytes correlates with cytoplasmic accumulation of glycogen granules and lipid droplets. Histological examination of hematoxylin and eosin (H&E)-stained wild-type and VHL-knock out liver sections revealed that cytoplasm of the adult liver cells became transparent within a week following VHL deletion both before and after fasting (Fig. 3A). This change was also observed in the new-born $VHL^{+F/+F}$/Albumin-$Cre^{+/-}$ pups, whose VHL gene in the liver is deleted when they are in the embryonic stages, and was partially ascribed to hepatocellular steatosis (10). Similar to the developing liver, VHL deletion in the adult mice led to accumulation of fat within the hepatocytes, as demonstrated with oil-red O staining (Fig. 3B). We also investigated whether there is alteration in the glycogen metabolism in VHL knock-out liver, as lack of cytoplasmic staining often reflects glycogen accumulation (16). Direct glycogen assay of the livers collected from starved animals showed that the total amount of glycogen per gram of tissue was much higher in the VHL knock-out liver than in the wild-type counterpart (Fig. 3B). The mice with VHL-deficient liver have a significantly lower serum glucose level than the wild-type mice (Fig. 3C). These data indicate that VHL plays

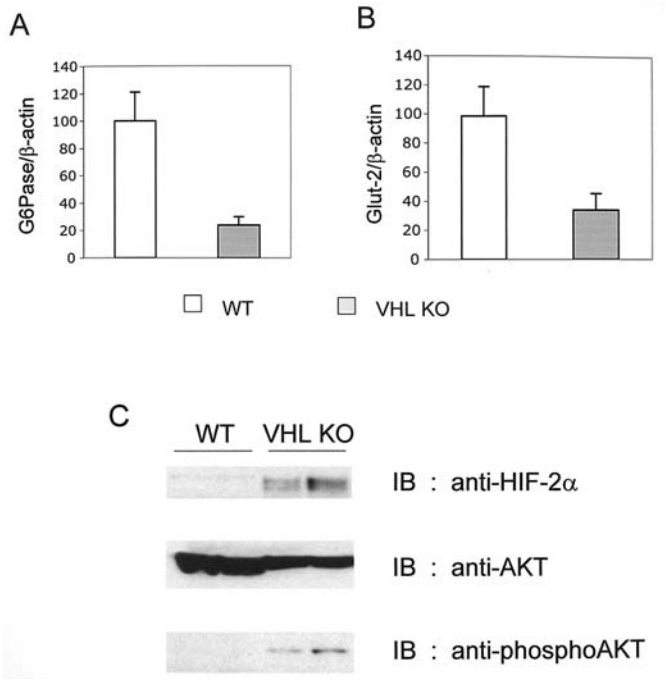

Figure 4. Reduced expression of glycogen metabolizing enzymes in VHL-inactivated liver. Glucose-6-phosphatase (A) and GLUT2 (B) mRNAs were measured by reverse-transcription coupled real-time PCR analysis with the primer sets shown in Table I. Each signal was normalized against ß-actin. The values for the mean ± SEM were calculated from 5 mice for each genotype and shown in the y-axis. (C) Western blot analysis of cell extracts shows sustained activation of AKT in VHL-inactivated liver. Top panel, increased expression of HIF-2α protein in VHL-inactivated liver. Middle panel, no significant effect on expression level of total AKT protein by VHL gene deletion. Bottom panel, sustained increase in activated form of AKT in VHL knock-out liver. Samples from two different mice for each genotype are shown.

an important role in liver glucose disposal and storage and inactivation of VHL results in accumulation of glycogen, which is an additional factor that causes clear cytoplasm in VHL-inactivated hepatocytes.

Inactivation of VHL leads to down regulation of genes involved in glucose metabolism. Glycogen metabolism in the liver is under the control of complex signaling networks reflecting various aspects of nutrition and hormonal status (17). In humans, several genetic locations are linked to abnormal hepatic glycogen metabolism, which are referred to as glycogen storage diseases (GSDs) (18). The fact that the phenotype of the VHL-inactivated liver closely resembles that of these human patients led us to investigate whether VHL regulates any of the genes affected in GSD. It has been well documented that deficiency of G-6-Pase is the genetic cause of human type I glycogen storage disease (18). Similarly, homozygous or compound heterozygous mutations of GLUT2 is known to cause a rare type of glycogen storage disease, named Fanconi-Bickel syndrome (FBS, OMIM 227810) in humans (19). By using reverse transcription-quantitative PCR (RT-qPCR) analysis, we examined the mRNA expression of these two GSD-associated and liver-specific genes (18). Interestingly, in the VHL KO hepatocytes, the expression level of G-6-Pase was much lower than in the wild-type liver (approximately 25% compared to the wild-type) (Fig. 4A). Ablation of VHL also led to a dramatic decrease in GLUT2 gene expression in hepatocytes (Fig. 4B). G-6-Pase catalyzes dephosphorylation of glucose-6-phosphate, which is an essential step for the release of either newly synthesized or glycogen-derived glucose from the hepatocytes (20), whereas GLUT2, characterized by low-affinity and high capacity, is a primary isoform of glucose transporter family expressed in the liver (21). In the aggregate, down-regulation of these two glucose metabolizing genes hampers proper release of glucose from the liver, resulting in abnormal hepatic accumulation of glycogen and hypoglycemia in VHL-deficient mice.

Increased phosphorylation of AKT in VHL-inactivated hepatocytes. Many phenotypes of the mice with VHL-inactivated liver, such as fatty liver, accumulation of glycogen and hypoglycemia, were also reminiscent of those of mice that express constitutively active AKT (i.e., myristoylated AKT) (22). This prompted us to examine the expression level and activation status of PKB/AKT in the VHL knock-out liver. First, we examined the total protein content of PKB/AKT in the whole cell extracts of both wild-type and VHL knock-out mouse livers and found that it was not affected by VHL deletion (Fig. 4C). However, the amount of activated form of PKB/AKT was significantly elevated in the VHL KO liver compared to the wild-type liver, as determined by Western blot analysis with phospho-specific anti-AKT antibody (Fig. 4C). These data indicate that the absence of functional VHL in the hepatocytes does not affect the level of PKB/AKT *per se*, but constantly activates PKB/AKT via phosphorylation, which in turn contributes to glycogen accumulation in the hepatocytes. As expected, HIF-2α protein level was increased dramatically in the nuclear extracts of VHL knock-out liver even without any hypoxic treatment (Fig. 4C).

Discussion

In order to gain further insight into the function of the VHL gene and acute effect of VHL inactivation in adult animals, we generated an inducible conditional VHL knock-out mouse model. This model allowed us to examine the cellular changes occurring shortly after loss of functional copies of the VHL gene in adult mouse liver and to identify novel functions of the VHL gene in hepatic glucose homeostasis. Quantitative analysis of glycogen content in the adult liver revealed that VHL inactivation leads to abnormal glycogen accumulation in hepatocytes. Furthermore, with real-time PCR gene expression analysis, we demonstrated that ablation of the VHL gene leads to down-regulation of GLUT2 and G-6-Pase gene expression in the liver. A causal link between these two genes and abnormal hepatic glycogen accumulation has been well-established in human glycogen storage diseases (19,20). In addition, studies with GLUT2-deficient mice had underscored the importance of GLUT2 in hepatic glucose homeostasis and provided a molecular explanation for how the lack of functional GLUT2 can lead to elevated glycogen storage in the liver (23). In these mice, mobilization of glycogen stored in the liver during the fasting period was significantly slowed down compared to that of wild-type control liver, increasing the steady-state level of cellular glycogen in the liver (23). Therefore, it is conceivable that downregulation of GLUT2

and G-6-Pase causes sustained accumulation of glycogen, rendering clear cytoplasmic characteristics in typical H&E staining of VHL-inactivated cells.

The best characterized gene expression change that occurs in VHL-inactivated cells is the transcriptional induction of glycolytic enzymes and pro-angiogenic factors (2,3). We also observed that HIF-dependent transcriptional activation is intact in VHL-inactivated hepatocytes, as evidenced by >100-fold induction of EPO expression and several fold induction of classical hypoxia-inducible genes, such as PGK, GLUT1, and VEGF. At present, it is unclear how both transcription induction and repression can occur simultaneously in the VHL-inactivated hepatocytes. One obvious question would be whether suppression of GLUT2 and G-6-Pase expression in VHL-inactivated hepatocytes is dependent on HIF-α. Ebert *et al* have demonstrated that hypoxia and hypoxia-mimicking chemicals, such as cobaltous ion or an iron chelator, exert opposite effects on gene expression of different isoforms of glucose transporters: hypoxia and hypoxia-mimetics enhance expression of GLUT-1 and GLUT-3, whereas they suppress expression of GLUT-2 in human hepatocarcinoma cell lines (24). This isoform-specific gene expression pattern of glucose transporters in hypoxic cells is strikingly similar to what we observed in VHL-deleted livers, which have increased expression of GLUT1 but decreased level of GLUT2. The fact that both genetic and pharmacological models for HIF-α activation produce a similar isoform-specific gene expression pattern for glucose transporters strongly supports the involvement of HIF-α in down-regulating GLUT2 and possibly G-6-Pase in VHL-inactivated liver cells. If this is indeed the case, HIF-α is likely to adopt a different pathway from the one that it relies on to up-regulate classical hypoxia inducible genes, such as EPO, VEGF, and more importantly GLUT1. Recently, two independent groups showed that hypoxia-induced cell cycle arrest can be at least partially explained by the antagonistic effect of activated HIF-1α on Myc-dependent transcription repression of cyclin-dependent kinase inhibitor, *p21cip1* (25,26). This cross-talk requires neither transcriptional nor DNA binding activity of HIF-1α toward the *p21cip1* promoter, but rather relies on direct protein-protein interaction involving the N-terminal half of HIF-1α (25,26). More importantly, this 'counteractive' function of HIF-1α in Myc-mediated gene expression also applies to the opposite gene regulation context, i.e. it is also capable of inhibiting the expression of genes, normally positively regulated by Myc, such as hTERT, BRCA1, and MSH2 and 6 (26,27). Interestingly, forced expression of Myc in the mouse liver selectively increases the expression of GLUT2, but not that of GLUT1 (28). Therefore, it is possible that, at least in part, overexpressed HIF-α in VHL-inactivated liver interferes with transcriptional activation by Myc at the GLUT2 promoter, thereby decreasing GLUT2 expression level. However, caution should be made to generalize this hypothesis to other GLUT2 expressing cells, because overexpression of Myc is sufficient to suppress GLUT2 expression in pancreatic ß cells (29). Nonetheless, it would be of interest to determine whether in fact HIF inhibits expression of GLUT2 by antagonizing Myc signaling in a certain type of VHL-inactivated cells. However, we do not exclude the possibility that VHL and/or HIF-α controls some other factors to maintain glucose flux in the liver. GLUT2 expression is also known to be positively regulated by other transcriptional factors, such as HNF-1α and SREBP-1c (30,31). Since both HIF and HNF-1 depend on p300/CBP for their transcriptional stimulation, it is also possible that the activated HIF represses gene expression through an indirect mechanism via competition with other GLUT2-inducing transcription factors (e.g., HNF-1α) for a common nuclear co-activator, p300/CBP (32).

Increased glycogen accumulation is also observed in the mice that express constitutively activated AKT (22). Several lines of evidence have suggested that activated AKT can repress expression of glucose metabolizing enzymes, including G-6-Pase, in both a forkhead transcription factor (FKHR)-dependent and -independent manner (33-35). Our finding that VHL deletion increases the level of phosphorylated AKT without any effect on the expression level strongly suggests that clear cytoplasm, increased glycogen storage, and decreased expression of G-6-Pase and GLUT2 in the VHL-inactivated hepatocytes result from AKT activation. Therefore, it would be very interesting to determine whether VHL can control any AKT upstream signaling molecules. Sustained activation of AKT has been implicated in various aspects of carcinogenesis (36). Clearly, extensive accumulation of cytoplasmic glycogen due to AKT activation would be restricted to glycogenic tissues, such as liver, muscle, and kidney, etc. However, it is plausible to hypothesize that the pVHL signaling pathway negatively targeting AKT exists in other non-glycogenic tissues, exerting different cell-type specific responses upon VHL inactivation in the course of VHL tumorigenesis. Further studies aimed at characterizing the molecular events that underlie AKT activation and down-regulation of GLUT2 and G-6-Pase in VHL-inactivated hepatocytes will shed more light on our understanding of VHL as a tumor suppressor and its roles in VHL syndromes.

Acknowledgements

The authors thank Wayne McNulty for technical assistance.

References

1. Lonser RR, Glenn GM, Walther M, Chew EY, Libutti SK, Linehan WM and Oldfield EH: von Hippel-Lindau disease. Lancet 361: 2059-2067, 2003.
2. Kaelin WG Jr: Molecular basis of the VHL hereditary cancer syndrome. Nat Rev Cancer 2: 673-682, 2002.
3. Semenza GL: Regulation of mammalian O2 homeostasis by hypoxia-inducible factor 1. Annu Rev Cell Dev Biol 15: 551-578, 1999.
4. Kaelin WG: Proline hydroxylation and gene expression. Annu Rev Biochem 74: 115-128, 2005.
5. Ratcliffe PJ: New insights into an enigmatic tumour suppressor. Nat Cell Biol 5: 7-8, 2003.
6. Gnarra JR, Zhou S, Merrill MJ, Wagner JR, Krumm A, Papavassiliou E, Oldfield EH, Klausner RD and Linehan WM: Post-transcriptional regulation of vascular endothelial growth factor mRNA by the product of the VHL tumor suppressor gene. Proc Natl Acad Sci USA 93: 10589-10594, 1996.
7. Iliopoulos O, Levy AP, Jiang C, Kaelin WG Jr and Goldberg MA: Negative regulation of hypoxia-inducible genes by the von Hippel-Lindau protein. Proc Natl Acad Sci USA 93: 10595-10599, 1996.
8. Zbar B and Lerman M: Inherited carcinomas of the kidney. Adv Cancer Res 75: 163-201, 1998.
9. Shiao YH, Kamata SI, Li LM, Hooth MJ, DeAngelo AB, Anderson LM and Wolf DC: Mutations in the VHL gene from potassium bromate-induced rat clear cell renal tumors. Cancer Lett 187: 207-214, 2002.

10. Haase VH, Glickman JN, Socolovsky M and Jaenisch R: Vascular tumors in livers with targeted inactivation of the von Hippel-Lindau tumor suppressor. Proc Natl Acad Sci USA 98: 1583-1588, 2001.
11. Kuhn R, Schwenk F, Aguet M and Rajewsky K: Inducible gene targeting in mice. Science 269: 1427-1429, 1995.
12. Cramer T, Yamanishi Y, Clausen BE, Forster I, Pawlinski R, Mackman N, Haase VH, Jaenisch R, Corr M, Nizet V, Firestein GS, Gerber HP, Ferrara N and Johnson RS: HIF-1alpha is essential for myeloid cell-mediated inflammation. Cell 112: 645-657, 2003.
13. Dobrzynski E, Montanari D, Agata J, Zhu J, Chao J and Chao L: Adrenomedullin improves cardiac function and prevents renal damage in streptozotocin-induced diabetic rats. Am J Physiol Endocrinol Metab 283: E1291-E1298, 2002.
14. Park SK, Dadak AM, Haase VH, Fontana L, Giaccia AJ and Johnson RS: Hypoxia-induced gene expression occurs solely through the action of hypoxia-inducible factor 1alpha (HIF-1alpha): role of cytoplasmic trapping of HIF-2alpha. Mol Cell Biol 23: 4959-4971, 2003.
15. Iliopoulos O, Ohh M and Kaelin WG Jr: pVHL19 is a biologically active product of the von Hippel-Lindau gene arising from internal translation initiation. Proc Natl Acad Sci USA 95: 11661-11666, 1998.
16. Emile JF, Lemoine A, Azoulay D, Debuire B, Bismuth H and Reynes M: Histological, genomic and clinical heterogeneity of clear cell hepatocellular carcinoma. Histopathology 38: 225-231, 2001.
17. Tirone TA and Brunicardi FC: Overview of glucose regulation. World J Surg 25: 461-467, 2001.
18. Wolfsdorf JI, Weinstein DA: Glycogen storage diseases. Rev Endocr Metab Disord 4: 95-102, 2003.
19. Santer R, Schneppenheim R, Dombrowski A, Gotze H, Steinmann B and Schaub J: Mutations in GLUT2, the gene for the liver-type glucose transporter, in patients with Fanconi-Bickel syndrome. Nat Genet 17: 324-326, 1997.
20. Van SE and Gerin I: The glucose-6-phosphatase system. Biochem J 362: 513-532, 2002.
21. Olson AL and Pessin JE: Structure, function, and regulation of the mammalian facilitative glucose transporter gene family. Annu Rev Nutr 16: 235-256, 1996.
22. Ono H, Shimano H, Katagiri H, Yahagi N, Sakoda H, Onishi Y, Anai M, Ogihara T, Fujishiro M, Viana AY, Fukushima Y, Abe M, Shojima N, Kikuchi M, Yamada N, Oka Y and Asano T: Hepatic Akt activation induces marked hypoglycemia, hepatomegaly, and hypertriglyceridemia with sterol regulatory element binding protein involvement. Diabetes 52: 2905-2913, 2003.
23. Burcelin R, del Carmen MM, Guillam MT and Thorens B: Liver hyperplasia and paradoxical regulation of glycogen metabolism and glucose-sensitive gene expression in GLUT2-null hepatocytes. Further evidence for the existence of a membrane-based glucose release pathway. J Biol Chem 275: 10930-10936, 2000.
24. Ebert BL, Gleadle JM, O'Rourke JF, Bartlett SM, Poulton J and Ratcliffe PJ: Isoenzyme-specific regulation of genes involved in energy metabolism by hypoxia: similarities with the regulation of erythropoietin. Biochem J 313: 809-814, 1996.
25. Mack FA, Patel JH, Biju MP, Haase VH and Simon MC: Decreased growth of Vhl-/- fibrosarcomas is associated with elevated levels of cyclin kinase inhibitors p21 and p27. Mol Cell Biol 25: 4565-4578, 2005.
26. Koshiji M, Kageyama Y, Pete EA, Horikawa I, Barrett JC and Huang LE: HIF-1alpha induces cell cycle arrest by functionally counteracting Myc. EMBO J 23: 1949-1956, 2004.
27. Koshiji M, To KK, Hammer S, Kumamoto K, Harris AL, Modrich P and Huang LE: HIF-1alpha induces genetic instability by transcriptionally downregulating MutSalpha expression. Mol Cell 17: 793-803, 2005.
28. Valera A, Pujol A, Gregori X, Riu E, Visa J and Bosch F: Evidence from transgenic mice that myc regulates hepatic glycolysis. FASEB J 9: 1067-1078, 1995.
29. Laybutt DR, Weir GC, Kaneto H, Lebet J, Palmiter RD, Sharma A and Bonner-Weir S: Overexpression of c-Myc in beta-cells of transgenic mice causes proliferation and apoptosis, downregulation of insulin gene expression, and diabetes. Diabetes 51: 1793-1804, 2002.
30. Ban N, Yamada Y, Someya Y, Miyawaki K, Ihara Y, Hosokawa M, Toyokuni S, Tsuda K and Seino Y: Hepatocyte nuclear factor-1alpha recruits the transcriptional co-activator p300 on the GLUT2 gene promoter. Diabetes 51: 1409-1418, 2002.
31. Im SS, Kang SY, Kim SY, Kim HI, Kim JW, Kim KS and Ahn YH: Glucose-stimulated upregulation of GLUT2 gene is mediated by sterol response element-binding protein-1c in the hepatocytes. Diabetes 54: 1684-1691, 2005.
32. Arany Z, Huang LE, Eckner R, Bhattacharya S, Jiang C, Goldberg MA, Bunn HF and Livingston DM: An essential role for p300/CBP in the cellular response to hypoxia. Proc Natl Acad Sci USA 93: 12969-12973, 1996.
33. Schmoll D, Walker KS, Alessi DR, Grempler R, Burchell A, Guo S, Walther R and Unterman TG: Regulation of glucose-6-phosphatase gene expression by protein kinase Balpha and the forkhead transcription factor FKHR. Evidence for insulin response unit-dependent and -independent effects of insulin on promoter activity. J Biol Chem 275: 36324-36333, 2000.
34. Barthel A, Schmoll D, Kruger KD, Bahrenberg G, Walther R, Roth RA and Joost HG: Differential regulation of endogenous glucose-6-phosphatase and phosphoenolpyruvate carboxykinase gene expression by the forkhead transcription factor FKHR in H4IIE-hepatoma cells. Biochem Biophys Res Commun 285: 897-902, 2001.
35. Lochhead PA, Coghlan M, Rice SQ and Sutherland C: Inhibition of GSK-3 selectively reduces glucose-6-phosphatase and phosphoenolypyruvate carboxykinase gene expression. Diabetes 50: 937-946, 2001.
36. Altomare DA and Testa JR: Perturbations of the AKT signaling pathway in human cancer. Oncogene 24: 7455-7464, 2005.